Supplemental Materials for "Topological surface states variation of MgB_2 after absorbing hydrogen, hydroxide, and water"

Pangdong Zhu,[1] Kun Bu,[2,*] Ruzhi Wang,[1] and Changhao Wang[1,†]

[1] *Key Laboratory of Advanced Functional Materials, Education Ministry of China, Faculty of Materials and Manufacturing, Beijing University of Technology, Beijing 100124, China*
[2] *School of Physics and Optoelectronic Engineering, Shandong University of Technology, Zibo 255000, China*

I. Wannier tight-binding model for MgB_2

In order to further explore the topological electronic properties of MgB_2, we have constructed the tight-binding (TB) model based on the s and p orbitals of Mg and B using the maximally localized Wannier functions implemented in the Wannier90 code [1, 2]. Fig. S1(a) shows the calculated TB band structures comparing with band structures calculated using the density functional theory (DFT), The TB and DFT band structures show a good match, thus confirming the validity of our Wannier TB models. Fig. S1(b) shows the nodal lines derived from the TB band structures, the six equivalent nodal lines can been seen clearly.

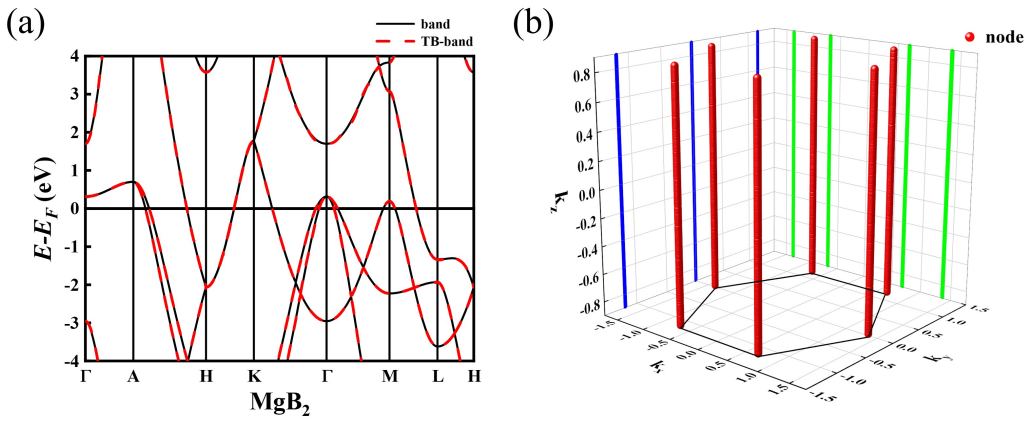

FIG. S1: (a) The tight-binding (TB) band structures in comparison with band structures derived from density functional theory (DFT). (b) The six equivalent nodal lines derived from the tight-binding band structures.

*e-mail address:bukun94@163.com
†e-mail address:wangch33@bjut.edu.cn

II. The effects of SOC on the energy band

Since Mg and B elements are light and SOC effects are weak, the influence of SOC was ignored in the study. As shown in FIG. S2, we compared the bulk phase band structure of MgB_2 with and without SOC, and found that SOC had almost no effect on the band structure. Therefore, SOC was not considered in the subsequent study.

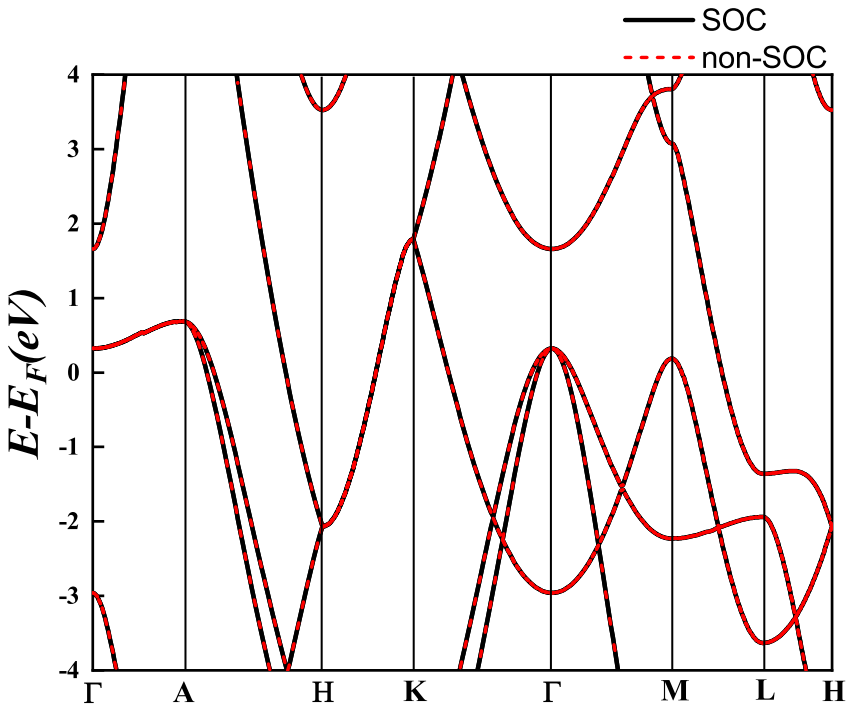

FIG. S2: The comparison of energy band calculation considering SOC and non-SOC for bulk MgB_2 material is presented (The red dashed lines are band maps considering SOC and the black lines are non-SOC.

III. Surface state analysis of multilayer structures

When building slab models, we tried to use 3-layer, 7-layer, 13-layer and 20-layer slab models to calculate the energy band structure, and found that the energy band structure reached stability after the 13th layer. Considering the saving of computing resources and the improvement of scientific research efficiency, we chose the 20-layer slab model for research. As shown in Figure S3 and S4, the slab band structures of the Mg/B end face of MgB_2 are 3, 7, 13 and 20 layers.

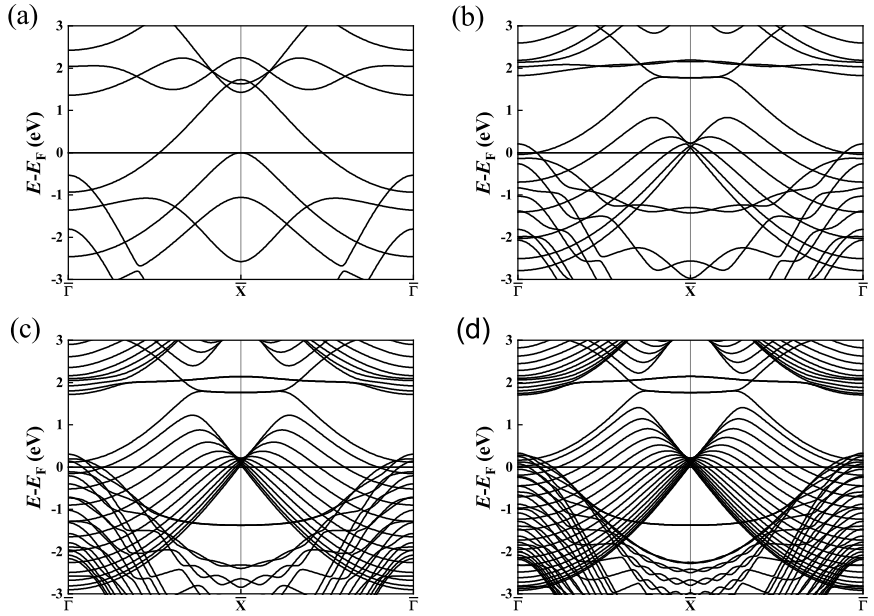

FIG. S3: Band structure of MgB_2 (010) Mg-terminated slab with (a) 3 layers; (b) 7 layers; (c) 13 layers; (d) 20 layers.

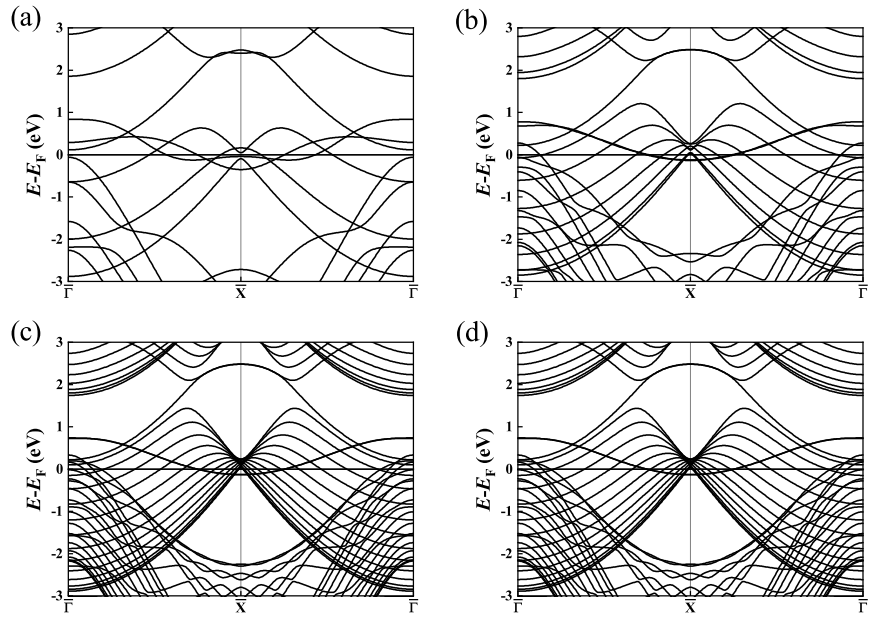

FIG. S4: Band structure of MgB_2 (010) B-terminated slab with (a) 3 layers; (b) 7 layers; (c) 13 layers; (d) 20 layers.

IV. The surface absorption Gibbs free energies at all possible absorption sites

TABLE S1: The surface absorption Gibbs free energy ΔG_{H^*} at all possible absorption sites for Mg/B-terminated slab models. Thermal Corrections at 300K.

	slab (eV)		slab+H (eV)	H_2 (eV)	ΔE_{H^*} (eV)	Thermal Corrections (eV)	ΔG_H (eV)
010-Mg	-288.18	bridge-1	-290.932	-6.696	0.596	0.132	0.728
	-288.18	bridge-2	-290.819	-6.696	0.709	0.097	0.806
	-288.18	top	-290.276	-6.696	1.252	0.084	1.336
	-288.18	hole	-292.02	-6.696	-0.492	0.173	-0.319
010-B	-296.524	bridge-1	-299.454	-6.696	0.418	0.1	0.518
	-296.524	bridge-2	-299.893	-6.696	0.418	0.1	0.518
	-296.524	top	-301.343	-6.696	-1.471	0.219	-1.252
	-296.524	hole	-298.923	-6.696	0.949	0.08	1.029

TABLE S2: The surface absorption Gibbs free energy ΔG_{OH} at all possible absorption sites for Mg/B-terminated slab models. Thermal Corrections at 300K.

	slab (eV)		slab+OH (eV)	OH (eV)	H_2 (eV)	H_2O (eV)	E_{OH} (eV)	Thermal Corrections (eV)	ΔG_{OH} (eV)
010-Mg	-290.316	bridge-1	-301.852	-7.097	-6.696	-14.223	-0.661	0.314	-0.347
	-290.316	bridge-2	-301.532	-7.097	-6.696	-14.223	-0.341	0.282	-0.059
	-290.316	hole	-301.248	-7.097	-6.696	-14.223	-0.057	0.221	0.164
	-290.316	top	-300.598	-7.097	-6.696	-14.223	0.593	0.284	0.877
010-B	-298.734	bridge-1	-308.725	-7.097	-6.696	-14.223	0.884	0.280	1.164
	-298.734	bridge-2	-310.064	-7.097	-6.696	-14.223	-0.455	0.294	-0.161
	-298.734	hole	-308.046	-7.097	-6.696	-14.223	1.563	0.234	1.797
	-298.734	top	-311.347	-7.097	-6.696	-14.223	-1.973	0.396	-1.442

TABLE S3: The surface absorption Gibbs free energy ΔG_{H_2O} at all possible absorption sites for Mg/B-terminated slab models. Thermal Corrections at 300K.

	slab (eV)		slab+H_2O (eV)	H_2O (eV)	E_{H_2O} (eV)	Thermal Corrections (eV)	ΔG_{H_2O} (eV)
010-Mg	-290.316	bridge-1	-304.639	-14.223	-0.1	0.54	0.44
	-290.316	bridge-2	-304.352	-14.223	0.187	0.542	0.729
	-290.316	hole	-304.336	-14.223	0.203	0.478	0.681
	-290.316	top	-304.74	-14.223	-0.201	0.519	0.318
010-B	-298.734	bridge-1	-312.728	-14.223	0.229	0.548	0.777
	-298.734	bridge-2	-312.672	-14.223	0.285	0.521	0.806
	-298.734	hole	-312.683	-14.223	0.274	0.536	0.81
	-298.734	top	-313.654	-14.223	-0.697	0.527	-0.17

In Table S1, S2, and S3, we have listed the surface absorption Gibbs free energies $\Delta G_{H,OH,H_2O}$ for all possible absorption sites at the Mg/B-terminated slab models, respectively. For Mg-terminated slab models, the most favorable absorption site for H is the hole site, for OH is the bridge site, and for H_2O is the top site; for B-terminated slab models, the most favorable absorption site for H is the top site, for OH is the top site, and for H_2O is the top site.

V. Fatband analysis for slab adsorbing H, OH, and H_2O

In Fig. S5, S6, and S7, we show the fatband analysis for Mg/B-terminated slab adsorbing H, OH, and H_2O, respectively. For Mg-terminated slab models, in all cases the topological surface state exists between two nodes; for B-terminated slab models, the topological surface state position changes when H and OH are adsorbed on the surface, while H_2O adsorption remains between the two nodes.

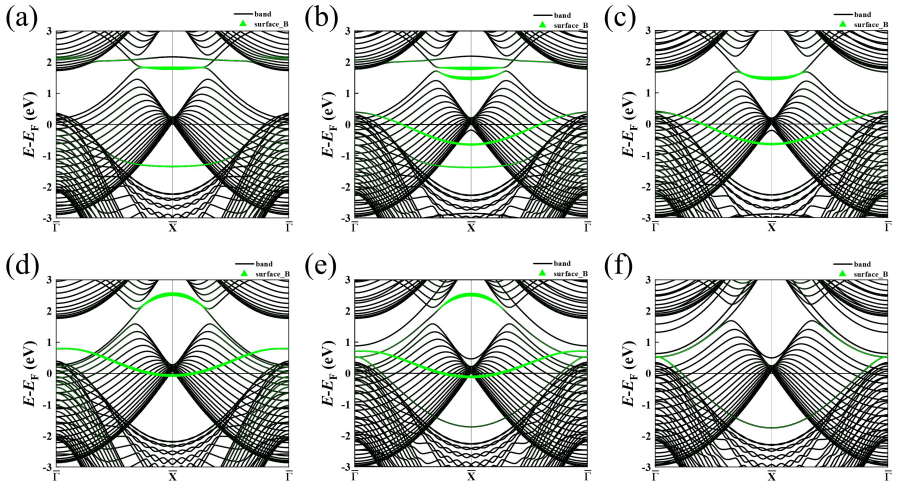

FIG. S5: (a) The (010) surface states given by the pristine Mg-terminated slab; (b) The (010) surface states given by the Mg-terminated slab adsorbing H on a single side; (c) The (010) surface states given by the Mg-terminated slab adsorbing H on both sides; (d) The (010) surface states given by the pristine B-terminated slab; (e) The (010) surface states given by the B-terminated slab adsorbing H on a single side; (f) The (010) surface states given by the B-terminated slab adsorbing H on both sides. The green triangles show the weight of the top layer of B atomic orbital states.

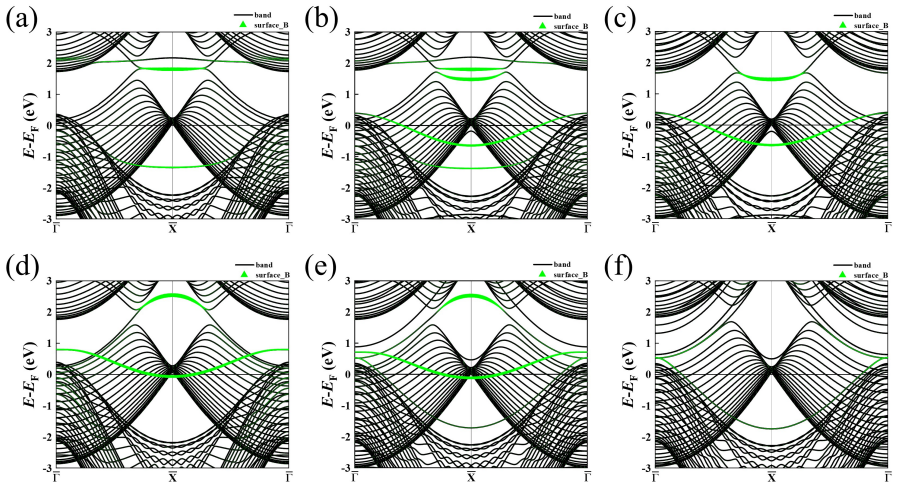

FIG. S6: (a) The (010) surface states given by the pristine Mg-terminated slab; (b) The (010) surface states given by the Mg-terminated slab adsorbing OH on a single side; (c) The (010) surface states given by the Mg-terminated slab adsorbing OH on both sides; (d) The (010) surface states given by the pristine B-terminated slab; (e) The (010) surface states given by the B-terminated slab adsorbing OH on a single side; (f) The (010) surface states given by the B-terminated slab adsorbing OH on both sides. The green triangles show the weight of the top layer of B atomic orbital states.

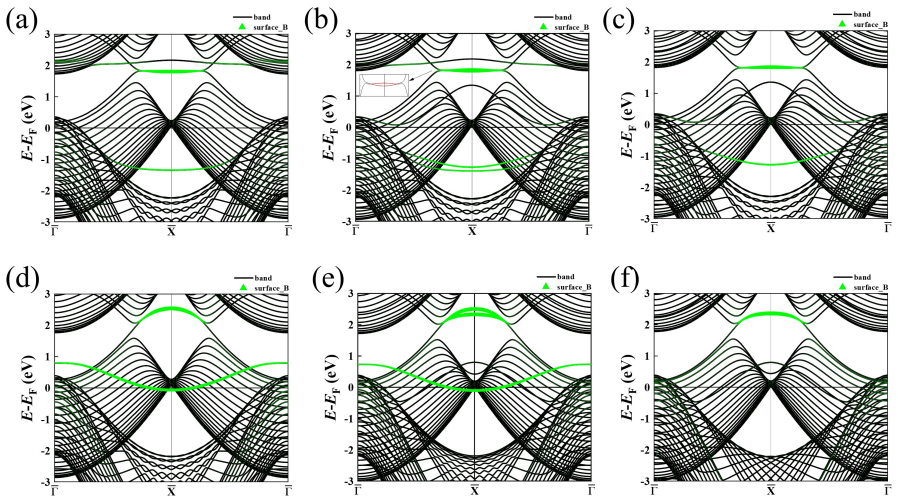

FIG. S7: (a) The (010) surface states given by the pristine Mg-terminated slab; (b) The (010) surface states given by the Mg-terminated slab adsorbing H_2O on a single side; (c) The (010) surface states given by the Mg-terminated slab adsorbing H_2O on both sides; (d) The (010) surface states given by the pristine B-terminated slab; (e) The (010) surface states given by the B-terminated slab adsorbing H_2O on a single side; (f) The (010) surface states given by the B-terminated slab adsorbing H_2O on both sides. The green triangles show the weight of the top layer of B atomic orbital states.

VI. Differential charge density for most favorable adsorption sites

Our calculations show the most favorable adsorption site for H, OH, H_2O is on the Mg/B-terminated slab of MgB_2. Under this state, we provide the map of the charge density difference as shown in Fig. S8. We find sizable charge depletion on the (010) surface of MgB_2 (see the bule field), which has transferred to adatom (see the yellow field).

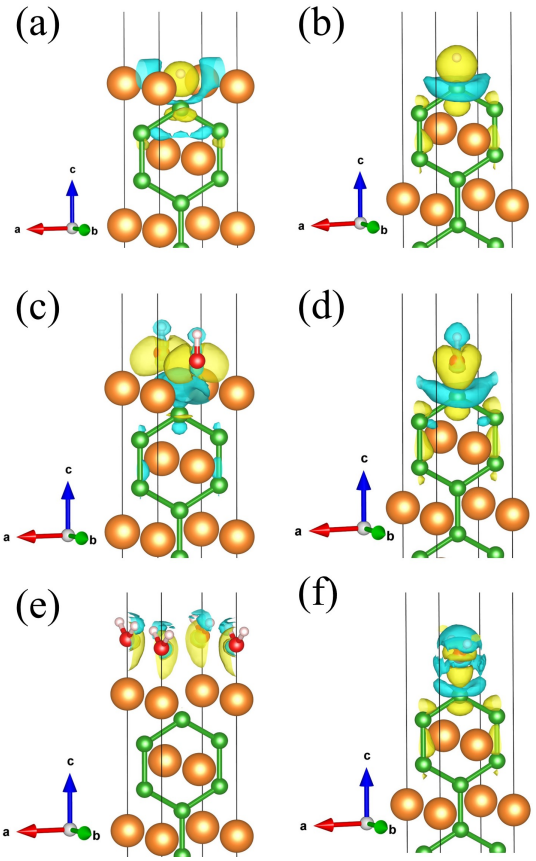

FIG. S8: (a) The Mg-terminated slab model after adding H on the hole site; (b) The B-terminated slab model after adding H on the top site; (c) The Mg-terminated slab model after adding OH on one bridge site; (d) The B-terminated slab model after adding OH on the top site; (e) The Mg-terminated slab model after adding H_2O on the top site; (f) The B-terminated slab model after adding H_2O on the top site. Meanwhile, we also show the band decomposed charge density of the surface bands at the projected $\overline{X}$ point. Yellow and blue represent the electron depletion and accumulation, respectively. The isosurface is taken as 0.003 electrons/$Å^3$.

VII. Relationship between bond distance, ΔG and ΔE_{TSS}

We further plotted ΔG and ΔE_{TSS}, as well as the bond distance of the adsorbate from the (010) surface of MgB_2 versus ΔE_{TSS}, as shown in Fig. S9. It can be seen that neither ΔG nor bond distance has a good linear relationship with ΔE_{TSS}.

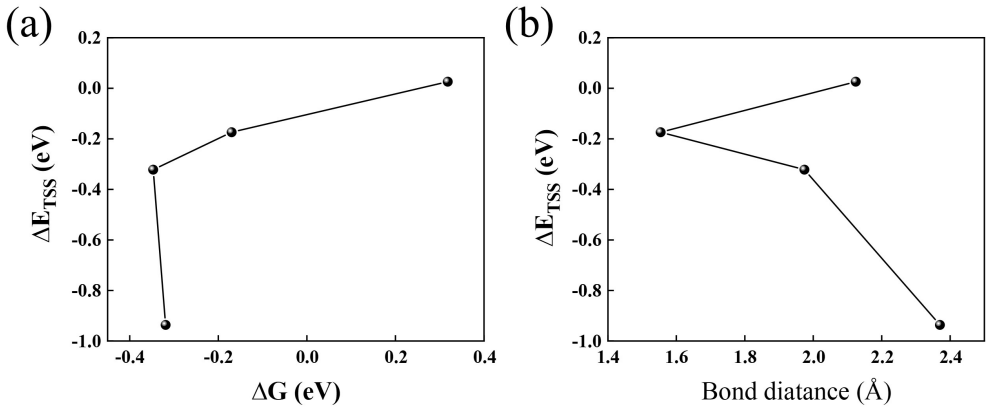

FIG. S9: (a) Topological surface state change and bond distance relationship; (b) Topological surface state change and $\Delta G_{\mathrm{H}^*,\mathrm{OH}^*,\mathrm{H_2O}^*}$ relationship.

[1] A. A. Mostofi, J. R. Yates, Y. S. Lee, I. Souza, D. Vanderbilt, and N. Marzari, *Wannier90: A tool for obtaining maximally-localised Wannier functions,* Comput. Phys. Commun. **178,** 685 (2008).
[2] N. Marzari, A. A. Mostofi, J. R. Yates, I. Souza, and D. Vanderbilt, *Maximally localized Wannier functions:Theory and applications,* Rev. Mod. Phys. **84,** 1419 (2012).